Ocean Engineering 216 (2020) 107843

Contents lists available at ScienceDirect

Ocean Engineering

journal homepage: www.elsevier.com/locate/oceaneng

Ship anemometer bias management

Eric Thornhill [a,*], Alanna Wall [b], Sean McTavish [b], Richard Lee [b]

[a] Defence Research and Development Canada, Canada
[b] National Research Council Canada, Canada

ARTICLE INFO

Keywords:
Anemometer bias
Sea trial
Ship wind measurements
Relative wind
Model tests
Wind tunnel

ABSTRACT

Wind measurements made on ships are used for general navigation, maritime operations, and in some cases logged to support oceanographic research. They are particularly important for aircraft-carrying ships as operations can be restricted in certain wind conditions. Shipboard wind measurements are subject to biases and inaccuracies as a result of air flow changing as it passes over and around the ship, its structures, and features. Ship-induced wind distortion and the resulting bias on anemometer readings can range from insignificant to severe. Anemometer bias cannot be completely eliminated for all conditions, but it can be managed so that reliable and accurate assessments of wind at sea can be identified. This paper describes the basic concepts related to ship wind distortion along with procedures and considerations on how bias can be quantified using simulations or model tests and validated using sea trials. An example case of a helicopter-carrying frigate is used to demonstrate the process of quantifying bias, calculating metrics, determining useful ranges, and developing and applying correction-functions. Wind tunnel measurements and a sea trial successfully demonstrated and validated the proposed ship anemometer bias management methodology.

1. Introduction

Wind measurements made on ships are subject to distortion as the air flow moves over and around the ship. The degree of distortion depends on factors such as the wind angle and speed, ship geometry, and the location of the sensor. Wind measurements are not only used for general navigation but are often logged to provide data for oceanographic research. Wind measurements are particularly important for ships which launch and recover aircraft as these operations can be unsafe or unachievable in certain wind conditions. Ship-induced wind distortion cannot be eliminated, but steps can be taken to evaluate the extent to which measurements are biased and to develop a means to correct and/or otherwise manage the issue to ensure operators are presented with useful data on their wind environment.

The Royal Canadian Navy is in the process of a recapitalization involving a mid-life refit of its patrol frigates, the introduction of new marine helicopters, and the acquisition of three new classes of helicopter-carrying naval ship. Anemometer bias analysis and ship airwake studies for aircraft operations are being conducted for both existing and future ships. This is to ensure accurate wind data are available to operators and that airwake characteristics will be suitable for a broad wind envelope for aircraft. This paper describes the methods used in these studies along with guidelines for evaluation and use that are generally applicable to naval and commercial vessels alike. Taken together, these processes are referred to as Anemometer Bias Management (ABM) and are used to ensure reliable wind readings at sea.

This paper begins with an overview of the distorting effect of bodies on the flow and a literature review of the work previously performed on ship ABM, followed by a discussion of modelling and validation techniques for evaluating wind bias. Design guidelines and considerations are then given along with general strategies for managing ship anemometer bias.

2. Flow distortions around ships

The measurement and understanding of flow distortions around ships is essential for managing the biases that affect ship anemometer readings. Bluff bodies modify the incoming flow in one or more of the following ways. Due to skin friction, flow moving along the surface of a body will be slowed near the surface, resulting in a boundary layer (Fig. 1(a)). The shape of the body may also induce changes in flow direction (Fig. 1(b)) or speed (Fig. 1(c)). For these first three distortion types, the flow is said to be attached, with the flow remaining largely in the freestream direction with the unsteady characteristics mainly unchanged. If the flow encounters a rapid change in body shape, depending on the shape and the pressure gradient on the body surface, the flow may separate which results in a shear layer (Fig. 1(d))

* Corresponding author.
E-mail address: eric.thornhill@forces.gc.ca (E. Thornhill).

https://doi.org/10.1016/j.oceaneng.2020.107843
Received 10 January 2020; Received in revised form 6 July 2020; Accepted 21 July 2020
Available online 14 September 2020

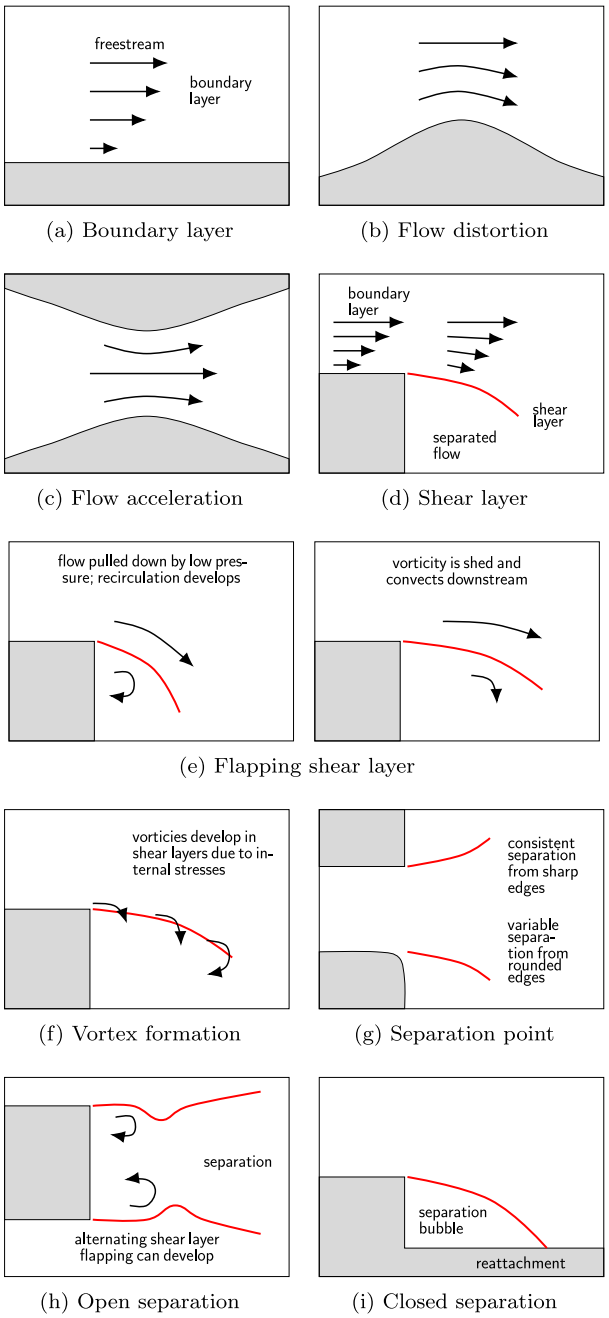

Fig. 1. Characteristics of bluff body flow distortion (arrows point in direction of flow).

where the flow speed changes rapidly from the freestream speed to a region of velocity deficit and recirculation behind the body. Shear layers flap in space and time (Fig. 1(e)) and promote the development of vortices due to the change in speed (Fig. 1(f)). Shear layers separate more consistently from sharp-edged objects than from round edges (Fig. 1(g)).

Flow separations are characterized by increased levels of vorticity and turbulence. An open separation (Fig. 1(h)) results in a turbulent wake. Depending on the geometry of the bluff body, a separated flow may be subject to reattachment and a closed separation that results in a separation bubble (Fig. 1(i)).

Conservatively speaking, a flow can be considered to be unaffected by a bluff body at a distance greater than 10 characteristic body dimensions away from the body. Therefore, any practical anemometer placement will be subject to biases induced by the overall ship superstructure and hull. This concept is illustrated in Fig. 2. In addition, biases are also induced by smaller features, such as masts or other ship-mounted equipment, within 10 characteristic lengths of the anemometer position. Since practical anemometer positions will undoubtedly be subject to biases, a practical goal of placement is ensuring that the biases are consistent across a range of operating conditions, and that they are unique — meaning the true flow can be calculated from the measurement, if bias characteristics are known.

The topology of the flow around a ship is governed by the non-dimensional Reynolds number,

$$\mathrm{Re} = \frac{\rho V L}{\mu} \tag{1}$$

where,

ρ is the flow density;
V is the characteristic flow speed;
L is the characteristic body dimension; and
μ is the flow dynamic viscosity.

The characteristic body dimension is the dimension that dominates the development of the flow topology. For example, in the case of a circular cylinder, the diameter is the characteristic dimension, even though the length may be much greater. In the case of a backwards-facing step (which leads to a separation bubble), the characteristic dimension is the step height. The characteristic flow speed should be close to the speed that dominates the development of the flow topology. For bluff body flow studies, the characteristic flow speed is usually the reference flow speed measured in the absence of the bluff body. The height of the reference speed also needs to be specified for bluff body aerodynamics applications near the surface of the earth due to the atmospheric boundary layer (ABL) (see Section 5.2). The ABL results from the same physical causes as the flow shown in Fig. 1(a).

The Reynolds number is the ratio of the inertial forces to the viscous forces in the flow. The drag forces on a bluff body, and the subsequent wake topology, are nominally dependent on the Reynolds number. Low Reynolds number flows (laminar regime) are characterized by gradual changes in forces with changes in Reynolds number. The transitional range of Reynolds numbers is associated with rapid changes in forces and flow topology with changes in Reynolds number. High Reynolds number flows (turbulent flow regime) are characterized by a general insensitivity to further changes in Reynolds number. These ranges are illustrated in Fig. 3, showing a typical relationship shape for circular cylinders.

The surface roughness, body shape, incoming flow turbulence level, and other factors influence the Reynolds numbers over which the three flow regimes (laminar, transitional, turbulent) are present. Of particular importance for ship airwake or anemometer studies is the Reynolds number where the flow can be assumed to be fully turbulent at full scale and also for testing at model scale to ensure similarity. Broadly speaking, separations from sharp edges and/or large features (such as the deck edge, the hangar, the bow) are less sensitive to Reynolds number than separations from rounded or small features (such as posts, lattice masts, fences) because the flow topology is more dependent on the shape of the body than on the flow itself. For ship airwake studies involving the flow in proximity to the flight deck, a lower Reynolds number limit of 11,000 (using the beam as the characteristic dimension) is typically used for Reynolds similitude, assuming the ship is largely sharp-edged (Healey, 1992). By comparison, flow over a cylinder is usually considered to be dependent on Reynolds number up to a value of 10^6. As a result, the study of anemometer biases requires a more subtle understanding of Reynolds number effect since anemometers are often placed within 10 characteristic body dimensions of round ship features and equipment. Unstable flow topologies for some wind conditions may render anemometer biases inconsistent and therefore unusable or uncorrectable.

Reynolds number effects are a fundamental aspect of modelling, measurement, and interpretation of anemometer biases, which will be

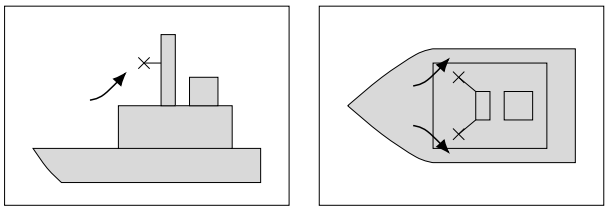

(a) Vertical flow distortion (b) Lateral flow distortion

Fig. 2. Graphical representation of flow distortions at anemometer locations (arrows point in direction of wind flow).

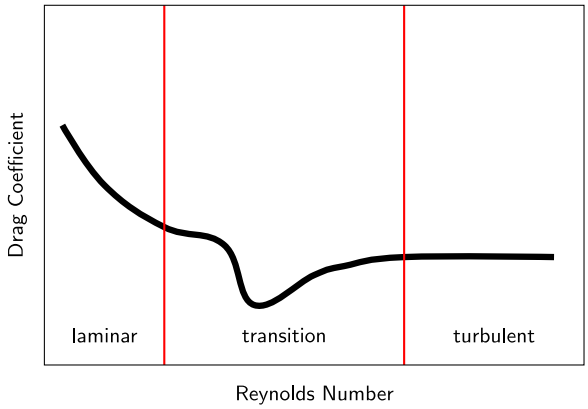

Fig. 3. Conceptual representation of variation in force coefficients with Reynolds number for bluff bodies (characteristics for smooth circular cylinder shown).

discussed at length in this paper. An understanding of the topological stability of the air flow is needed if model-scale or shipboard measurements are to be interpreted properly.

3. Wind: definitions and conventions

Wind direction in this paper adheres to the convention used in meteorology and by mariners. It is the direction where the wind is *coming from*; e.g., a north wind is where the air moves from the north to the south and a starboard wind is where air moves from starboard to port. Consequently and unless specified otherwise, wind vectors[1] in the figures will point to the coming-from direction. Note that this approach is opposite to the convention used most in fluid dynamics where direction is defined by where the flow is *going to*.

Wind direction is given either with respect to the compass rose (e.g., 0° to 359°, where 0° is true north) or relative to the ship centreline; converting between the two references can be done using Eq. (2). When using a relative reference, the terms 'red' (R) and 'green' (G) winds refer to port and starboard winds, respectively, as shown in Fig. 4.

Although 3D effects of wind distortion can be significant for some anemometer placements, the vertical component of wind is rarely measured by ship's anemometers. Therefore only wind in the horizontal plane is considered.

$$\theta_W = \psi_W - \psi_H \tag{2}$$

where,

θ_W is the wind direction relative to the ship centreline;

[1] Even when explicitly using the coming-from convention, there is no consensus on how wind vector arrows should be oriented in diagrams. Depending on the context, arrows can either point to the wind's coming-from or going-to directions.

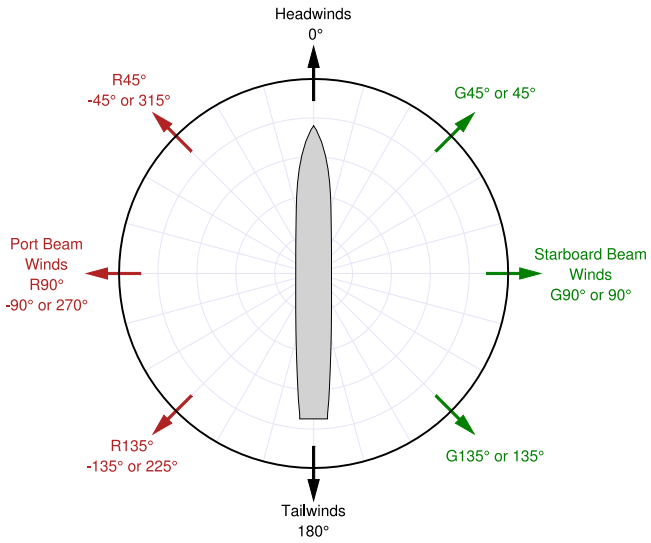

Fig. 4. Nomenclature for relative wind angles (arrows point to the direction that the wind is coming from). Winds from the starboard side are called 'green winds' and have angle values preceded by 'G'. Winds from the port side are called 'red winds' and have angle values preceded by 'R'. Headwinds and tailwinds refer to wind within ±5° of 0° and 180°, respectively.

ψ_W is the wind direction relative to true north;
ψ_H is the ship heading relative to true north.

Fig. 5 shows a diagram illustrating the various wind vectors, defined below, used in evaluating anemometer biases. From the perspective of a ship at sea, only two of these vectors are known initially; the ship generated wind $\vec{S}$ from the ship speed and course, and the measured wind $\vec{M}$ from the anemometer(s). The goal of bias management is to account for the distortions in $\vec{M}$, caused by the air moving over and around the ship to determine the corrected relative wind $\vec{C}$. As discussed in later sections, these vectors are functions of wind direction and height above sea level (and in some cases, wind speed).

True Wind: True wind, $\vec{T}$, is the ambient atmospheric wind flowing over the ocean surface. It has a vertical velocity distribution as a result of the ABL where wind speed increases with height above the water. Unless otherwise specified, true wind speed is given at the anemometer height.

Ship Generated Wind: Ship generated wind, $\vec{S}$, is created by the movement of the ship through still air. It is treated as an idealized concept where the ship has no effect on the air through which it moves. The ship generated wind speed is defined in Eq. (3) as the ship speed, V_S in the direction of the ship course over ground, ψ_C (using the 'coming from' convention).

$$\vec{S} \equiv V_S \angle \psi_C \tag{3}$$

Note the ship course, ψ_C does not always align with the ship heading ψ_H. The difference between them, called drift angle, can be substantial for certain operating conditions.

Undistorted Relative Wind: Undistorted relative wind, $\vec{U}$, is the idealized concept of relative wind as the vector sum of the true and ship generated winds. This is the relative wind that would be measured on a ship that had no effect on the air around it.

$$\vec{U} \equiv \vec{T} + \vec{S} \tag{4}$$

Measured Relative Wind: Measured relative wind, $\vec{M}$, is the wind as measured at a specific point on the ship. The measured relative wind is a combination of the true and ship generated winds, and also includes

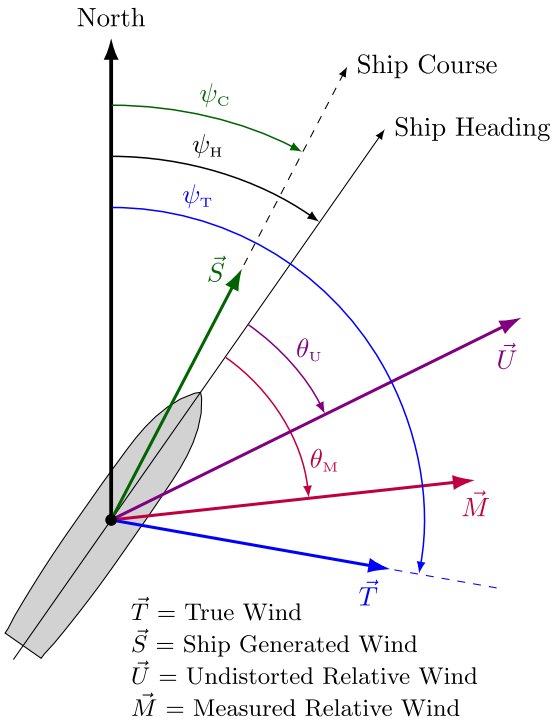

Fig. 5. Wind vector and angle (vectors point to the direction the wind is coming from).

all of the distortion effects caused as the air is forced to flow over and around the ship structures.

Corrected Relative Wind: Corrected relative wind, $\vec{C}$, is an estimate of the idealized undistorted wind $\vec{U}$ that is made by applying a correction (developed for example from wind tunnel data) to the measured wind $\vec{M}$. It is not always possible to apply corrections to $\vec{M}$.

$$\vec{C} \approx \vec{U} \tag{5}$$

4. Literature review

4.1. Preliminary measurements of bias effects on ships

Observations of distortions in wind measurements made from ships were reported as early as the mid-1960s. These observations came mostly from research vessels where measurements from the mast were compared with other sources such as nearby buoys or from shore-based sensors (Bogorodskiy, 1966; Augstein et al., 1974; Hoeber, 1977; Pierson, 1990). Bias effects at different locations on a ship were also observed through comparisons of wind measurements on a ship's mast and various extended booms (Ching, 1976; Kahma and Leppãranta, 1981; Kidwell and Seguin, 1978; Rahmstorf, 1989; Blunt, 1991). These effects were quantified through the use of scaled model wind tunnel tests, which estimated the flow distortion error at potential shipboard anemometer sites to be as large as 40 % (Elliot, 1981).

4.2. Ship wind measurement for oceanographic studies

A large focus of the published work for wind measurement bias on ships came from the scientists who use wind measurements (and other data) from thousands of ships globally as part of the World Meteorological Organization (WMO) Voluntary Observing Ships (VOS). There was enough distortion of meteorological measurements induced by ships that it was adversely affecting weather and sea state forecasts (Hoeber, 1977; Blanc, 1986b). The National Oceanography Centre (NOC) in Southampton, UK, has performed a considerable amount of work on the subject of ship anemometer speed bias which focused primarily on improving data from VOS for oceanographic studies. These studies include full-scale measurements from research vessels, wind tunnel model tests, and the use of computational fluid dynamics (CFD) to quantify ship-based anemometer bias (Moat, 1994; Taylor et al., 1999; Yelland et al., 2002; Moat, 2003; Moat et al., 2004b,a, 2005; Moat and Yelland, 2005; Moat et al., 2006b,a; Moat and Yelland, 2009).

Several of these studies consisted of steady-state CFD simulations to predict the speed biases for anemometers mounted on a mast located at the bow of the ship (Moat et al., 2006b; Moat and Yelland, 2009; Yelland et al., 2002). Additional series of CFD simulations were conducted to predict wind speed biases on generic container ships in order to improve the wind speeds reported by VOS. Simulations of generic container ships were used to develop predictions of wind speed bias as a function of bridge height in bow and beam winds. The speed bias on top of the bridge of these container models ranged from +11 % to −100 %, indicating that regions of flow acceleration and regions of reversed flow were present as a result of the bridge geometry. General guidance for anemometer positioning suggested by Moat et al. (2006a, 2005) included placement of anemometers in regions where shear is low, near the forward edge of large structures (such as the bridge), and to avoid regions where wakes are present.

Outside of the NOC, other researchers were also using CFD to evaluate flow distortions at ship anemometer positions in order to improve observation data. Popinet et al. (2004) presented results from a CFD study using the unsteady large-eddy simulation (LES) research code Gerris to investigate the characteristics of the mean airflow and the turbulent wake around the ship RV Tangaroa. Good agreement over a full range of relative wind angles was found between the simulations and measurements from a corresponding sea trial at several positions (in regions of both high and low flow distortion). They concluded that both the normalized wind speed and normalized standard deviation were only weakly dependent on wind speed, ship speed, ship motion, and sea state, but strongly dependent on relative wind angle. While anemometer placement does affect the dependence of anemometer readings on speed and motion-related factors, biases that depend on wind angle only are preferred.

O'Sullivan et al. (2013) presented results of a study using the CFD code OpenFOAM to simulate the errors in wind speed measurements caused by flow distortion on the RV Celtic Explorer and validated the predictions with full-scale data. Simulations were performed over a range of relative wind angles from R60° to G60° and velocities from 10 to 50 knots. The numerical results were within 12 % of experimental measurements, which could possibly be improved using different CFD processes specifically tuned for unsteady ship airwakes. It was also shown that although the wind angle is a dominant factor in flow distortion errors (Popinet et al., 2004; Yelland et al., 2002), these errors can also change as a function of wind speed magnitude due to Reynolds number effects.

O'Sullivan et al. (2015) present a study where results from the OpenFOAM Reynolds-averaged Navier–Stokes equations (RANS) solver SimpleFOAM and LES solver PisoFOAM are compared with experimental data taken from various anemometer sites onboard the RV Knorr. The LES produced mean accuracy levels of ~3 % of the wind speed bias whereas the RANS simulations produced mean accuracies of ~7 %. They also investigated two different methods to define a wave-induced flow distortion correction which was found to improve the overall accuracy of the models by up to 3 % (O'Sullivan et al., 2015).

4.3. Anemometer correction-functions

Much of the literature discussed so far, although investigating ship-induced bias on anemometer measurements, focused on improvements to oceanographic data sets generated by VOS. The focus of the current effort, however, is the improvement of wind measurements for the

ship operators while at sea. One way of doing this is by applying correction-functions to the wind data in real-time before it is shown on the ship displays. The following papers discuss the development of correction-functions for various ships.

For the LHA Tarawa Class, Blanc (1986a) estimated that the accuracy of the type of sensor used on the LHA was ±2 % for wind speed and ±3° for wind angle; this represented the best possible case in ideal conditions. However, wind tunnel tests demonstrated that wind measurements made at the standard anemometer locations could be in serious error due to flow distortions caused by the ship. For example, near the top of the forward-most mast, measurement errors were as much as 50 % for wind speed and greater than 10° for wind angle. The test conditions included neutral atmospheric stability, constant sea surface roughness, zero pitch and roll attitudes, no aircraft on the flight deck, and a motionless ship.

Blanc concluded that corrections are necessary in order to report undisturbed relative wind readings and that corrections should be specific to both the ship class and the anemometer locations because of the spatial variations of the flow around the ship. Furthermore, he proposed Blanc (1986b) that the wind speed measurement error could be minimized by developing correction algorithms for the standard anemometer locations on each class of ship based on measurements made with ship models in a wind tunnel.

The correction scheme presented by Blanc consisted of tables for each anemometer which listed the indicated relative wind angles in increments of 5°, followed by columns containing a wind speed correction and a wind angle correction. The corrected relative wind was then determined by the following equations.

$$\text{(Corrected RW Speed)} = \text{(Indicated RW Speed)} * \text{(Speed Correction)} \tag{6a}$$

$$\text{(Corrected RW Angle)} = \text{(Indicated RW Angle)} + \text{(Angle Correction)} \tag{6b}$$

The typical overall accuracy of the corrected values under a variety of environmental conditions, exclusive of any inherent sensor error, was estimated to be ±5 % for wind speed and ±5° for wind angle (Blanc, 1986a). It was noted that this approach could be easily adapted to an automated system that could compute and display the corrected readings on the bridge of the ship or wherever the information might be needed.

Similar reports were also made for the Virginia Class (Blanc, 1987) and Nimitz Class (Blanc and Larson, 1989). Although the values in the correction tables varied, the procedures and conclusions were effectively the same for all three ship classes.

Thiebaux (1990) presents the results of scale model tests for three research vessels, CSS Dawson, CSS Baffin, and CSS Hudson in a boundary-layer wind tunnel used to develop correction-functions for the shipboard anemometers. Measurements were performed at the ship anemometer locations as well as a bow reference location. Bow reference anemometers are often used for comparative measurements from which to assess anemometer biases. While still subject to flow distortions from the ship, bow anemometers placed above the bow separation region (if present) are subject to lower biases, smaller changes in biases with wind angle, and lower levels of superstructure-induced turbulence than their typical mast-mounted counterparts.

As was done by Blanc (1986a), the correction-functions developed by Thiebaux were presented in tabular form with columns for indicated relative wind angle (every 10°), angular correction, and speed correction (Thiebaux, 1990). Corrected relative wind could be determined from the indicated relative wind using appropriate table data and Eq. (6). This study revealed an issue with biased anemometer readings, where the same indicated wind angles were measured for different actual wind angles; this complicates the development of correction-functions as the correct angle was indeterminate with two or three possible solutions. This observation led to a requirement that anemometer measurements must be unique for a given wind angle.

US NAVAIR, who have extensive experience and established procedures for ABM, is a member of relevant NATO groups to which Canada also belongs. A current summary of their procedures is given in the report by NATO Advanced Vehicle Technology (AVT) working group AVT-217 (AVT-217 Task Group, 2015). In the open literature, Polsky et al. (2011) discuss a feasibility study for using CFD instead of wind tunnel testing for performing Anemometer Position Evaluations (APEs) for naval vessels. This is the process the United States Navy typically employs to determine the range of indicated winds for which the anemometers of a ship are useable for flight operations. A detailed description of an APE is given including the test matrix, instruments, and analysis procedure. Three metrics are used when generating anemometer useful-ranges (URs): speed distortion, angle distortion, and turbulence intensity. If the anemometer is in the wake of a large object for a given relative wind angle, then the location would likely have flow characteristics that would fail these metrics. The operators would then be instructed to disregard anemometer data for this region.

The focus of their study was to use CFD to perform an APE on two candidate vessels for which wind tunnel data existed, USNS Dahl and a Joint High Speed Vessel (JHSV). A discussion of the procedures was given and the results between the CFD and wind tunnel data were presented. Overall, the CFD results followed the trends of the wind tunnel data but could differ in absolute values depending on the specifics of each simulation.

5. Anemometer Bias Management

Anemometer Bias Management (ABM) is the process of ensuring reliable wind readings at sea. To be useful, anemometer readings do not need to be unbiased from flow distortions, but they do need to be consistent and unique.

5.1. Anemometer types

Common types of anemometers used on ships include: propeller–vane, cup–vane, 2D ultrasonic, and 3D ultrasonic.

Propeller/cup–vane units obtain the wind speed from the rate of propeller or cup rotation and wind direction from the vane angle. This method of measurement can result in some of the following issues:

- Inability to resolve horizontal wind speeds independent of vertical flow distortions that may be present at that location;
- Dynamic behaviour in unsteady winds leading to an incorrect measurement of unsteady flow characteristics;
- The potential for measurement characteristics to be influenced by ship motion;
- Phase lag behaviour; and
- Poor low speed response.

The fact that horizontal wind speed reported by these units can be influenced by the wind's vertical component presents an issue when attempting to compare measurements made in a wind tunnel to those from a ship fitted with propeller/cup–vane anemometers. An adjustment is needed to account for the vertical component's effect on the ship-fitted sensors. Such corrections are sometimes available from the manufacturer but in cases where they are not, an estimation can be used (for propeller–vane units) which models a theoretical response of rotors to vertical flow (Mazzarella, 1954). This correction, given by Eq. (7), is made by multiplying the 3D velocity magnitude V_{3D}, by the cosine-squared of the flow elevation angle, ϕ, to get an equivalent propeller–vane horizontal indicated speed, V_{pv}:

$$V_{pv} = V_{3D} \cos^2 \phi \tag{7}$$

where,

V_{pv} is the equivalent speed reported by the propeller–vane unit;
V_{3D} is the flow velocity magnitude including all three components; and
ϕ is the wind elevation angle.

Ultrasonic anemometers measure the wind speed based on the speed of an ultrasonic pulse travelling between a set of transducer heads, one for each direction component. As such, they are not subject to the limitations listed above. They are becoming more common for new installations and mid-life refits as they tend to be smaller, lighter, and provide more accurate wind information. However, ultrasonic anemometers can be susceptible to icing and corrosion, electromagnetic interference from nearby emitters, or from local temperature changes such as from the ship's exhaust.

5.2. Atmospheric boundary layer

The true wind over the surface of the Earth, $\vec{T}$, has a vertical velocity distribution called the atmospheric boundary layer (ABL) where wind closer to the sea surface is slower than wind higher up due to friction between the air and the ground/sea surface. The shape of the ABL depends on a number of factors, including surface roughness and the atmospheric stability. The vertical profile can be estimated by a variety of models (Forand, 2018), which can take some or all of these factors into account (Davenport, 1960). For anemometer bias analysis, a simple power-law estimate, Eq. (8), which is common for wind engineering studies and is given in the NATO standardized definitions[2] for wind and wave conditions (NATO, 1993) is often used.

The standard reference height for wind speeds used in the NATO document was $z_{ref} = 19.5\,\text{m}$; speeds at other heights are determined using Eq. (8). Unless otherwise indicated by a subscript, such as $\vec{T}_{19.5}$, wind speeds in this paper are given for the height of the anemometer.

$$T_B = T_A \left(\frac{z_B}{z_A} \right)^{\alpha} \tag{8}$$

where,

T_A is the known true wind speed at height z_A;
z_A is the vertical height above the nominal ocean surface corresponding to the known wind speed T_A;
z_B is the vertical height above the nominal ocean surface for which the true wind speed is desired;
T_B is the true wind speed at height z_B;
α is an empirically derived power law exponent. Ref. NATO (1993) specifies $\alpha = 1/7 \approx 0.14$, but ships at sea could experience profiles with α in the range of 0.09 to 0.25 (Davenport, 1960).

By definition, the undistorted relative wind, $\vec{U}$, is the vector sum of the true wind, $\vec{T}$ which follows a power-law distribution (left side of Fig. 6) and ship generated wind, $\vec{S}$, which has an idealized uniform distribution (right side of Fig. 6).

When $\vec{T}(z)$ and $\vec{S}(z)$ combine, the angle between them can introduce a twisting effect on the resultant vertical distribution of $\vec{U}(z)$. This is illustrated in Fig. 7 showing winds when a ship travels in a direction perpendicular to the true wind. Numerous combinations of $\vec{T}(z)$ and $\vec{S}(z)$ with varying speeds and angles could sum to give the same $\vec{U}$ at the anemometer height, but with different vertical profiles for $\vec{U}(z)$.

The shape of the ABL profiles can modify the development of the distorted flow fields around a ship, which may impact various aspects of operation differently. This issue primarily affects ships where the anemometers have been placed far from a height of interest (e.g., the helicopter hover height). Corrections made to determine wind conditions at the height of interest will be subject to uncertainties in wind speed and direction due to ABL variation.

[2] The equation is provided in the footnotes of Table D-1 of Ref. NATO (1993).

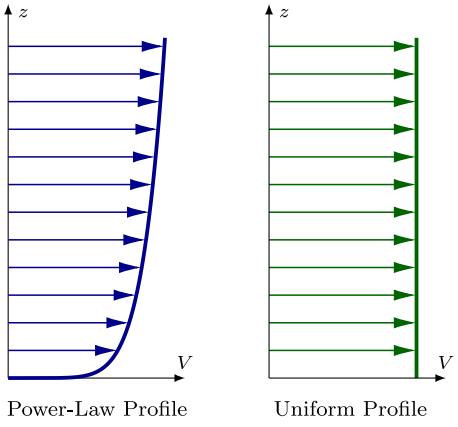

Fig. 6. Conceptual illustration of vertical velocity profiles.

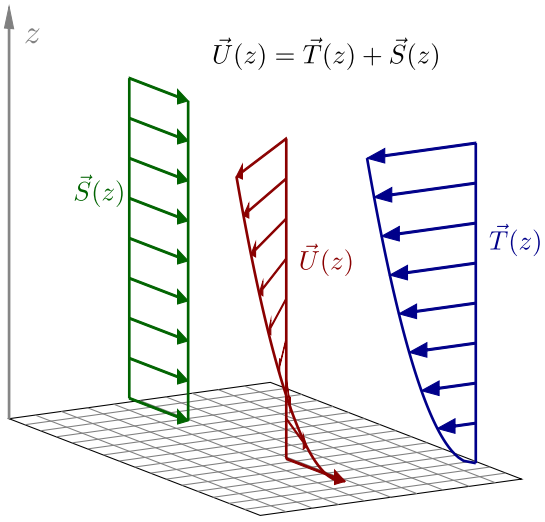

Fig. 7. Conceptual illustration of wind profiles combining to create a twisted profile.

This illustrates an aspect of anemometer bias management, where the details of the ship, operational need, and anemometer placement are extremely important in determining the best course of action.

5.3. Ship orientation and motion

Standard practice for anemometer bias tests is to use a level static ship and would therefore neglect any effects due to a tilted ship or one undergoing motions due to ocean waves.

In the case of a ship's orientation, the list or trim angle due to uneven loading would generally be small (a few degrees at most) and would not be expected to have a significant effect (i.e., less than the precision of the full scale sensors) on the wind distortion or measurement. The same would be true for modest changes in ship draft.

Ship motions due to sea states, however, can result in larger angles and dynamic effects which can affect both wind distortion and measurement. Large angles of roll and pitch can tilt the anemometer out of the horizontal plane, affecting which components of the wind are being measured. As most ship anemometers are only 2D, measurements cannot be properly corrected for out-of-plane measurements. A procedure to apply tilt corrections for anemometers was presented by Wilczak et al. (2001), though this was more applicable to non-shipboard installations.

Large angles also substantially change the shape of the ship presented to the wind; distortion effects and the resulting bias could

therefore be quite different for an even-keeled ship and one, for example, rolled over to 20°. Thiebaux (1990) tested models in both an even-keeled orientation and with static roll (20°) and pitch (5°) angles resulting in differing biases profiles for each condition; dynamic effects were not considered.

Rolling and pitching motions can also generate large velocities, particularly for anemometers located high up on a ship's mast. The movement of the anemometers through the air generates apparent wind velocities and the movement of the ship can generate dynamic wind distortions. Dynamic wind distortion is more complicated and would likely require ship-specific studies to quantify its effects. The influence of ship motion on wind measurements has been explored by Reinsvold (2013), but this type of analysis is not usually included in standard anemometer bias evaluations.

In practice, applying a low-pass filter to the anemometer data using a frequency lower than ship's natural frequencies of motion is often sufficient to remove (or reduce) these effects.

5.4. Anemometer location quality metrics

The quality of an anemometer location is assessed by measuring the biases and evaluating the mean and fluctuating component of the wind measured at the anemometer location that includes the distortion effects of the ship superstructures. A time series, x, of instantaneous measurements is collected in order to perform the analysis. The normalized mean wind speed (horizontal component), given by $\hat{x}$ and the normalized standard deviation (horizontal component), given by τ_x, are the typical assessment metrics for a given anemometer location.

$$\bar{x} = \frac{1}{n}\sum_{i=1}^{n}(x_i) \tag{9}$$

$$\hat{x} = \frac{\frac{1}{n}\sum_{i=1}^{n}(x_i)}{U_{\text{ref}}} \tag{10}$$

$$\tau_x = \frac{\sqrt{\frac{1}{n}\sum_{i=1}^{n}(x_i - \bar{x})^2}}{U_{\text{ref}}} \tag{11}$$

where,

- $\bar{x}$ is the mean of x for a given time series comprised of n discrete measurements;
- $\hat{x}$ is the normalized value of $\bar{x}$;
- n is the number of elements in the time series of x;
- U_{ref} is undistorted wind speed at a standard reference height;
- x_i is the i^{th} measurement in the series;
- τ_x is the normalized standard deviation of the fluctuating component of x.

The quality metrics used here are normalized by the undistorted wind speed at a standard reference height of 19.5 m, $U_{19.5}$. The height was selected to be consistent with the NATO reference wind height for sea state definition (NATO, 1993). This approach has been adopted by the co-authors as it facilitates the comparison of bias from ships that may have different anemometer heights. In other contexts, a different reference height may be more meaningful.

The qualities of a good anemometer location are:

- Insensitive to Reynolds number: which is indicated by stable values of $\hat{x}$ with wind speed; and
- Outside of wake regions and flapping shear layers: which is indicated by levels of τ_x which are on the order of the turbulence intensity in the undistorted atmospheric wind and also by low rates of change of $\hat{x}$ and τ_x with wind angle.

Statistics are expressed only for the horizontal component due to the fact that many measurement devices are limited in their measuring capability to the horizontal plane and the fact that the determination of undistorted wind, which is inherently horizontal, is the goal. The mean of the vertical distortion, if measured, can also indicate the level of flow distortion; however, the presence of vertical distortions is not necessarily an indicator of poor placement. Also, the unsteady component of the vertical distortion is unlikely to provide insight not already captured by the level of unsteadiness in the horizontal plane.

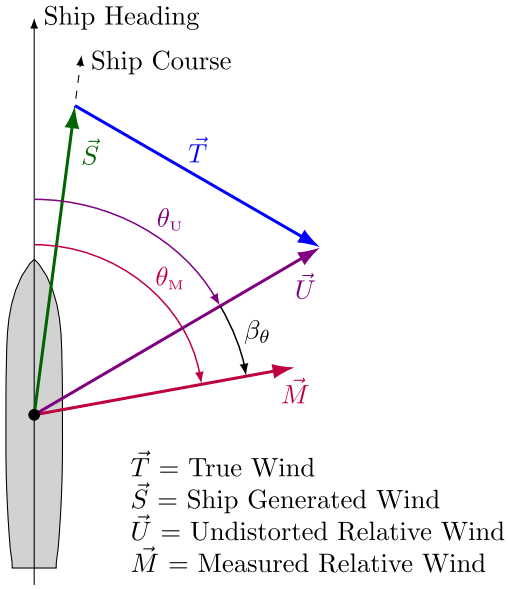

Fig. 8. Wind vector diagram (vectors point to the direction the wind is coming from).

5.5. Bias correction factors

Bias factors used both for defining the magnitudes of bias, as well as for their correction, are given in Eq. (12). The angular bias, β_θ, is the difference between the measured, $\vec{M}$, and undistorted, $\vec{U}$, wind angles and the speed bias, β_V is the ratio of the measured to undistorted wind speeds. Note that bias is a function of anemometer location, wind angle, and to some extent wind speed (see Section 6.1). The relationship between measured and undistorted winds is represented graphically in Fig. 8.

Note that variations of Eq. (12) could also be defined by reversing the order of $\bar{\theta}_{\text{M}}$ and $\bar{\theta}_{\text{U}}$ in Eq. (12a), and/or inverting the ratio in Eq. (12b). Other researchers have used these variations, such as Eq. (6) by Blanc (1986a).

$$\beta_\theta = \bar{\theta}_{\text{M}} - \bar{\theta}_{\text{U}} \tag{12a}$$

$$\beta_V = \frac{\bar{M}}{\bar{U}} \tag{12b}$$

where,

- $\bar{\theta}_{\text{M}}$ is the mean azimuth angle of $\vec{M}$ w.r.t. the ship centreline;
- $\bar{\theta}_{\text{U}}$ is the mean azimuth angle of $\vec{U}$ w.r.t. the ship centreline;
- $\bar{M}$ is the mean 2D horizontal wind speed of $\vec{M}$;
- $\bar{U}$ is the mean 2D horizontal wind speed of $\vec{U}$;
- β_θ is the anemometer angle bias correction;
- β_V is the anemometer speed factor correction.

5.6. Accuracy requirements

Anemometer measurements are subject to uncertainties resulting from a number of sources, including:

- Superstructure-induced biases;

- Aerodynamic uncertainties in biases (possible sources: Reynolds number sensitivity, sensitivity to the ABL); and
- Instrument uncertainties (possible sources: unexpected dynamic behaviour, alignment issues, instrument calibration and/or resolution, installation variation).

For example, uncertainty levels for wind measurements could be defined such that they must be no greater ±5° for wind angle, and ±2 knots for wind speed below 40 knots and ±5 % above 40 knots. Uncertainty targets should include both the accuracy of the installation and measurement uncertainties associated with the instruments used at sea.

6. Bias measurement considerations

The standard method for evaluating ship anemometer bias is through model scale testing in a wind tunnel and/or CFD simulations. The procedure is essentially the same in both cases. A representative version of the above-water geometry of the ship is generated. The model is then placed in the wind tunnel or computational domain and exposed to a range of known wind conditions while measurements are taken at the anemometer position(s). For each wind condition and location, the difference between the measured winds, $\vec{M}$, and the known undistorted winds $\vec{U}$ are then used to characterize the angle and speed biases.

The following sections describe the process in more detail and describe important considerations when making wind bias measurements including scaling, model fidelity, propeller–vane corrections, turbulence intensity, and the ABL.

6.1. Scaling

Achieving meaningful results from scale model tests requires that the experiments are designed to comply with the principles of similitude. As physical phenomena can be governed by different and sometimes opposing conditions for similitude, consideration should be given to ensure that behaviours of interest are being modelled correctly. For ship airwake studies, the similitude parameters required for dynamic and kinematic similitude, respectively, are Reynolds number, Re, defined in Section 2, and reduced frequency, f^*, as defined below.

$$f^* = \frac{\omega L}{V} \tag{13}$$

where,

f^* is the reduced frequency;
V is the wind velocity;
L is the characteristic body dimension; and
ω is frequency.

These two parameters cannot be matched simultaneously in a conventional atmospheric wind tunnel. However, as discussed in Section 2, dynamic similitude does not require Reynolds number matching if the flow is in a regime where the flow characteristics are consistent across the range of relevant Reynolds numbers both at model and full scale. At very low wind speeds Reynolds similitude cannot be maintained; therefore, a successful experimental design requires that this lower limit occurs below the scaled wind speed of interest. For ship airwake studies, a lower limit of 10 knots (full scale) is generally used, where the influence of wind at this speed on operations is limited.

The reduced frequency, f^*, is used to scale the relative frequencies for testing and analysis. By Eq. (13), for a reduced scale model, the frequencies of fluctuations in the flow (for the same wind speed) occur faster by the same amount. Eq. (14) illustrates the interplay between the three parameters: size, speed, and frequency, all of which can be manipulated to optimize the experimental design while maintaining kinematic similitude.

$$f_m^* = f_f^* \tag{14a}$$

$$\frac{f_m^*}{f_f^*} = \left(\frac{\omega_m}{\omega_f}\right)\left(\frac{L_m}{L_f}\right)\left(\frac{V_f}{V_m}\right) = \frac{\lambda_\omega \lambda_L}{\lambda_V} = 1 \tag{14b}$$

$$\lambda_L = \frac{L_m}{L_f} \tag{14c}$$

$$\lambda_V = \frac{V_m}{V_f} \tag{14d}$$

$$\lambda_\omega = \frac{\omega_m}{\omega_f} = \frac{\lambda_V}{\lambda_L} \implies \lambda_t = \frac{\lambda_L}{\lambda_V} \tag{14e}$$

where,

X_m, X_f are parameters X at model and full scale, respectively;
λ_L is the geometric scale factor;
λ_V is the wind velocity scale factor;
λ_ω is the frequency scale factor;
λ_t is the time scale factor.

The equations for reduced frequency scaling are relevant for ensuring sufficient sampling time and rate to capture the dominant effects of interest, and also for spectral analyses. Provided the tests are conducted in appropriate Reynolds number conditions then measurements of flow speed at anemometer locations can be normalized directly by the reference wind speed for the test point and no further scaling is required for stationary statistical quantities like mean and standard deviation.

6.2. Model fidelity

To minimize effort and cost, there is an incentive for both numerical and physical model testing to simplify the geometry of the ship model as much as possible. This is done by either excluding or reducing the complexity of details and features of the ship's structure. For these studies, it is acceptable to remove details on the order 1 m or less, unless these details are within 10 object dimensions of the anemometer position or could be reasonably expected to cast a significant wake on the anemometer for any relative wind angle.

Compound objects, such as lattice masts or multiple repeating instances of small objects can have an effective characteristic geometry that is on the order of the compound object rather than the individual pieces. In this case, the object should be treated as a porous object, where many studies estimating drag and wake topology for porous objects exist.

Due to Reynolds number effects on the individual elements of a compound object or objects where the Reynolds number regime at model scale is not representative of the full scale equivalent, geometric scaling does not always produce an equivalent flow structure. A model for equivalent drag must be developed using literature or testing of the object itself in order to accurately reproduce the flow effect of these types of objects at model scale. Therefore, the appropriate simplification of a ship geometry for adequate simulation requires judgement calls and experience to do correctly.

6.3. Atmospheric boundary layer

The simple power-law profile described in Section 5.2 using $\alpha = 1/7 \approx 0.14$ from NATO (1993) is considered sufficient for simulations of ship anemometer biases and can be generated using a series of triangular spires for wind tunnel tests (Irwin, 1979). A power-law profile with this coefficient value represents average conditions found at sea.

6.4. Sampling rates and durations

Ship-induced wind distortion is an inherently unsteady process involving turbulent flow fluctuations covering a broad range of length and time scales. Measurement of the wind therefore needs to be done

over a sufficient duration to extract meaningful statistics. The measurement technique, whether wind tunnel, at-sea, or CFD, impacts the appropriate duration.

Some preliminary estimations of the primary frequencies that may exist in the flow can be done using vortex shedding theory (Zdravkovich, 1997) from the ship as a whole and individually for its major structural features. A more practical approach though is to perform a sensitivity analysis on the measurement duration, to ensure that it is long enough to produce statistically significant mean and Root Mean Square (RMS) values.

The sampling rate for the measurements must be sufficient to resolve the time scales of interest. At the NRC wind tunnel, scale measurements supporting ship-helicopter operations are typically made at 5000 Hz – more than sufficient to capture turbulence frequencies related to ship anemometer bias. Measurement durations at model scale may theoretically only need to be a few seconds, but in practice wind tunnel data is normally collected for periods in the range of 10 to 30 s.

CFD simulations for anemometer bias should be performed as transient rather than steady-state. In this way the fluctuating components, which are used as metrics for evaluating bias, can be captured. Timestep size in CFD applications are driven by factors such as the numerical scheme and grid dimensions but should be at least small enough to capture frequencies of interest. Simulations also require some time for the flow to properly develop from its initial conditions at startup before measurements at anemometer positions should be made.

In the case of ship trials conducted at sea, marine anemometers typically report wind measurements at 1 Hz, though commonly-used ultrasonic sensors can go as high as 30 Hz. At sea, inherent turbulence in the ambient wind as well as ship motions can also affect measurement times. Depending on conditions, durations for trial measurements can be as low as 2 to 5 min, though for the dedicated trials discussed in Section 8, runs were each at least 15 min.

7. Anemometer bias analysis

7.1. Wind tunnel results

An example of wind tunnel results for anemometer bias and their use for ABM is given in this section. The selected case is the port side anemometer position of a Halifax Class frigate; this class of ship is fitted with two (port and stbd) anemometers near the top of its mast as shown Fig. 9.

The wind tunnel anemometer bias tests were conducted at the NRC 9 m Wind Tunnel facility in Ottawa using a 1:50 scale model of the ship mounted on a turntable, as shown in Fig. 10. Flow measurements at each anemometer location were taken using a single Cobra probe (see Fig. 11), suspended above the wind tunnel floor by a structure mounted downstream of the turn-table. A Cobra probe (Turbulent Flow Instrumentation, 2019) is a fast-response, four-hole pressure sensor that provides dynamic, three-component velocity and static pressure measurements within an acceptance cone of ±45°. The acceptance cone limits the range of measurement; for example, the probe as positioned for the test can only accurately measure flow vectors that are not distorted more than 45° vertically or horizontally from the probe tip's longitudinal axis.

The following procedure was performed for each of the anemometer locations. First, the three-component wind velocity was measured without the ship installed. This was done to determine the characteristics of the undistorted wind and the baseline turbulence intensity. Next, the model was positioned in the tunnel and the three-component wind velocity was measured at the anemometer position(s). The ship was then rotated w.r.t. the tunnel air flow direction using the turntable (to change θ_U) and the flow measurements were taken again.[3] This process

[3] The Cobra-probe sensor was always aligned to the wind tunnel flow direction and did not rotate with the ship.

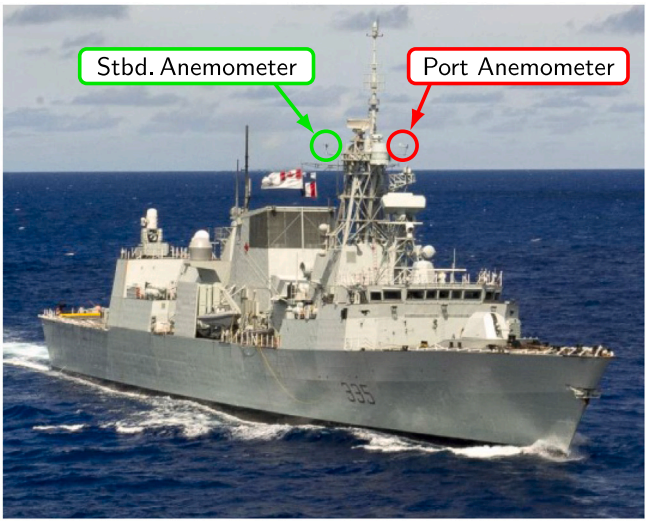

Fig. 9. Halifax Class frigate showing its port and starboard anemometers.

was repeated for the full range of relative wind angles. The Halifax Class used propeller–vane anemometers at the time of the wind tunnel testing, so the measured 2D wind speed results from the wind tunnel were adjusted for vertical velocity as described in Section 5.1.

The bias results and location quality metrics for the port anemometer are given in Fig. 12. The top two charts show the results for speed and angle bias calculated using Eq. (12). For winds coming to the port side (anemometer on windward side), there was some moderate direction bias of ±5° as well as a reduction in 2D wind speed by as much as 20 %. In port beam winds, the 2D horizontal speed decreases, but the normalized vertical velocity (bottom chart) increases. The total 3D wind speed would therefore increase in port winds due to the strong up-draft created as the wind is accelerated upward and over the broad side of the ship.

As can be seen in Fig. 9, the port anemometer is on the leeward side of the mast for starboard winds, and is in a wake region for certain relative wind angles. The wind tunnel results, particularly speed bias, clearly show this effect as the wind speed drops to nearly zero for starboard beam winds when the anemometer is leeward of the mast structure. The edges of the wake are characterized by the rapid changes in speed bias and the centre of the wake is characterized by the greatest velocity deficit.

Another important factor to consider is the turbulence intensity, τ_V using Eq. (11) shown in the fourth plot of Fig. 12; the data shown are for the difference in turbulence intensity, $\Delta\tau_V$ measured at the anemometer position from the baseline value taken in an empty tunnel. Large values of $\Delta\tau_V$ indicate that the wind flow is highly turbulent — in these cases, measurements may be unstable and consequently cannot be corrected. For the example data shown, the $\Delta\tau_V$ is low for port winds indicating stable and correctable bias. Higher and rapidly changing $\Delta\tau_V$ for starboard winds suggest more turbulent and unstable conditions, particularly in mast shear layers. Note that both the speed bias and turbulence metrics are needed for evaluation. For example, there are low turbulence levels in the centre of the wake at G90°, but this is simply a consequence of the nearly zero wind speed in the wake of the mast and not an indication that the measurements here are correctable.

7.2. Useful range

One of the primary objectives of ship anemometer bias analysis is to determine the useful range for when data can be used and when it should be discarded. It is important that operators are aware when sensor data is invalid due to excessive bias or instability. Useful

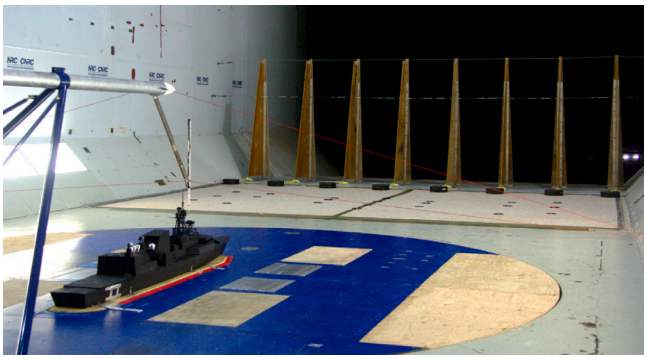

Fig. 10. Wind tunnel set-up for anemometer bias assessment on the Halifax Class. Flow conditioning devices (spires and carpet) can be seen upstream of the ship.

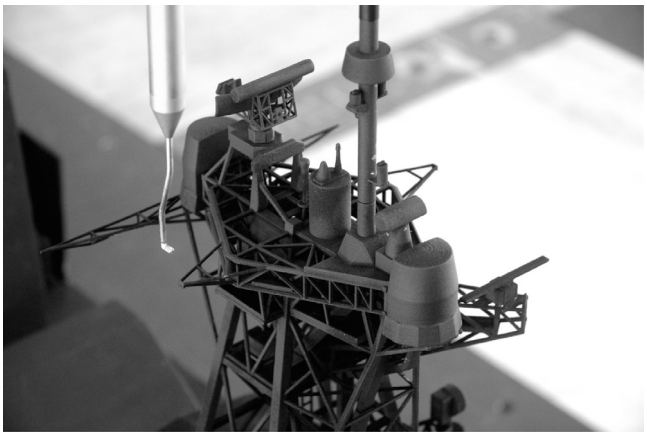

Fig. 11. Close-up view of Fig. 10 showing ship mast and Cobra probe.

data occur when the anemometer is in wind conditions that can produce consistent, repeatable measurements that are within, or can be corrected to be within, the required accuracy (see Section 5.6).

The specific criteria for defining useful range will depend on the requirements for the data, as well as the characteristics of the bias profile. For example, Polsky et al. (2011) uses criteria based on threshold values for β_θ, β_V, τ_V as well as their gradients. In general terms, anemometers should not be used if they are within or on the edge of separated flow regions with highly turbulent flow. These are typically seen, but not limited to, when the sensor is downwind of some object or structure. They can be identified by large values of turbulence intensity inside separated regions and large gradients in bias metrics at the edges.

For the data in Fig. 12, the useful range was defined as covering relative wind angles from G170° clockwise through all port wind angles to G10° as illustrated by Fig. 13. Although port beam winds did exhibit bias, the wind flow was stable (i.e., low values of τ) and therefore amenable to correction. In contrast, the majority of the starboard wind angles caused the sensor to be in lee of the mast and resulted in highly distorted and chaotic flows. This behaviour can be observed on the real ship; the leeward anemometer (propeller–vane type) will sometimes spin in circles in response to the mast's wake flow.

Ships should be fitted with anemometers located such that the combination of their useful ranges provides full coverage over 360° of undistorted wind angles. Overlap of useful ranges is recommended for best results. For the Halifax Class, the starboard anemometer data has a (mostly) mirror image bias profile as the port anemometer. It therefore has overlap for both headwinds and tailwinds so that together, both anemometers can provide the ship with full valid measurement coverage.

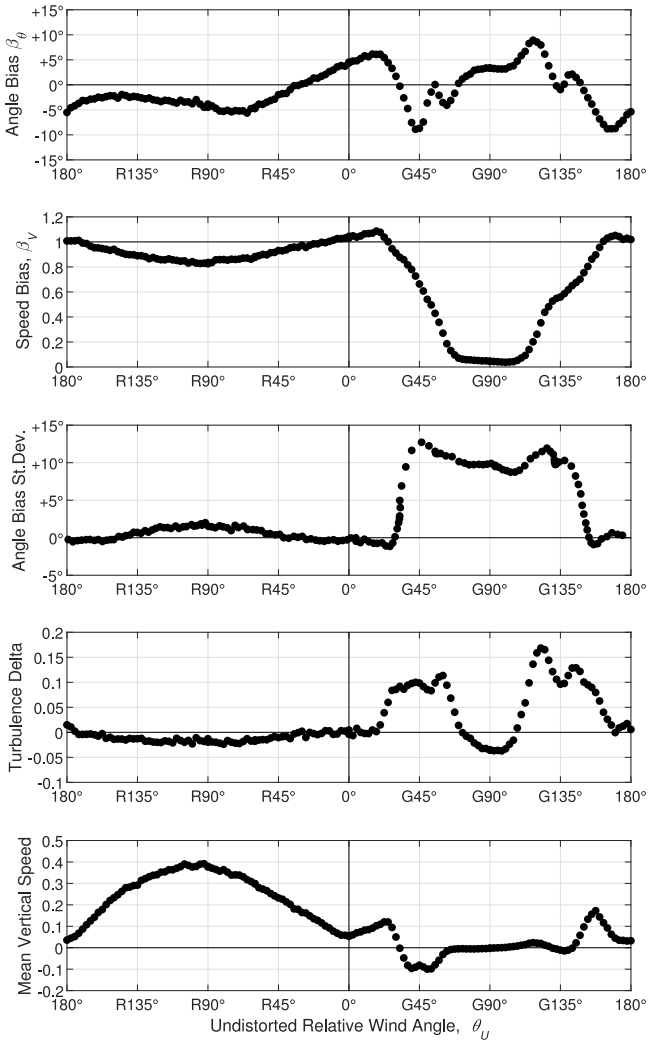

Fig. 12. Wind tunnel results for port side anemometer.

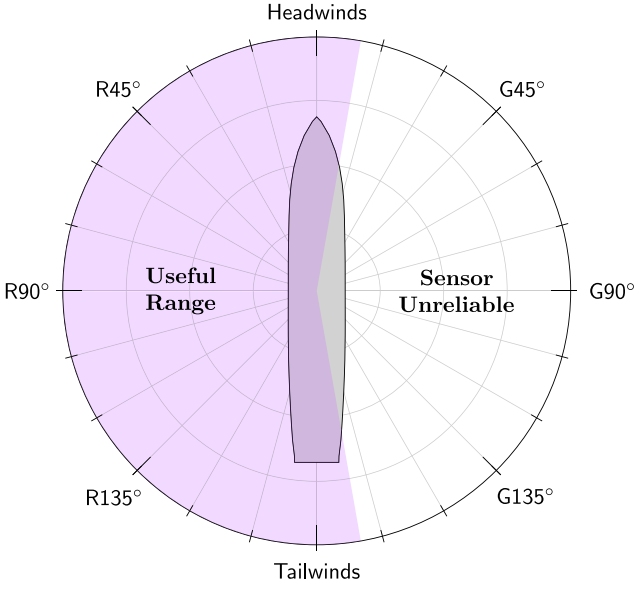

Fig. 13. Port anemometer useful range for the Halifax Class shown shaded.

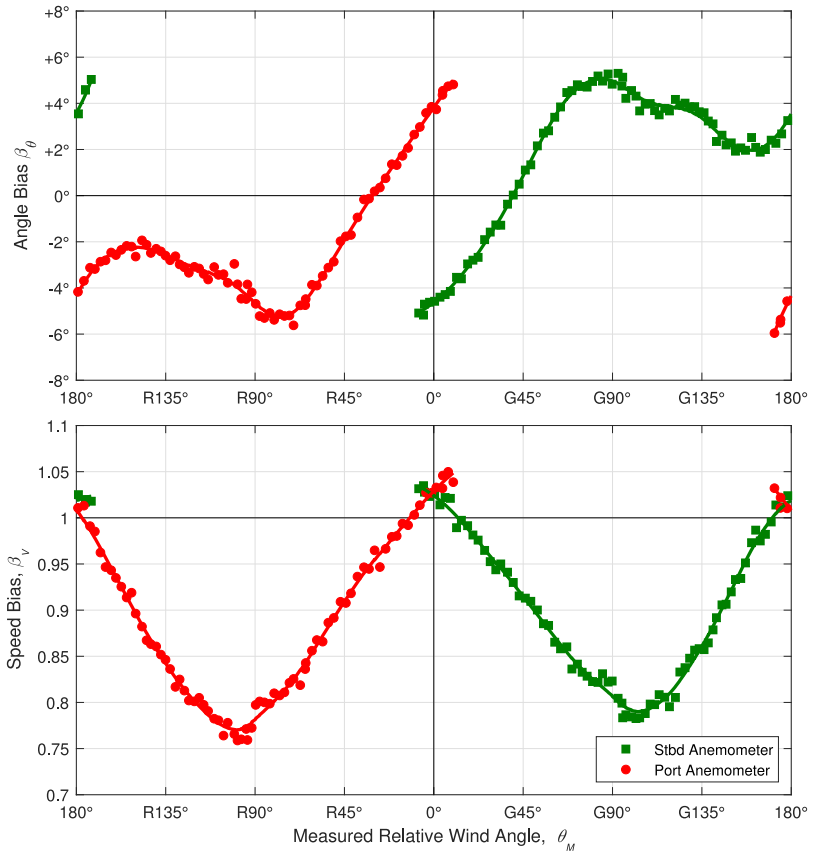

Fig. 14. Port and starboard anemometer biases plotted against measured wind angle.

7.3. Bias correction

If the airflow distortion to the anemometer is significant, it may be helpful to apply a correction to remove, or at least reduce, the resulting bias. This can be done by using the same data from Fig. 12 but truncated to the useful range and plotted against θ_M instead of θ_U. Fig. 14 shows this version of the data along with that collected for the starboard anemometer; smooth curves are also fitted to each data set.

The bias correction procedure would be to first check that the measured angle is within the anemometer's useful range, then to use the fitted curves from Fig. 14 to determine the relevant speed and angle bias, then to apply Eq. (12) to calculate θ_U and U.

Applying these corrections can avoid ambiguity from sensors that have different bias profiles. Using the current example for headwinds, the port anemometer would measure G5° while the starboard anemometer measures R5°, but the corrected values would be consistent.

7.3.1. Anemometer selection

Although seemingly straight-forward, bias correction has a complication where incorrect data can be displayed. This is when an anemometer is outside of its useful range in terms of the undistorted wind angles (θ_U), but due to it being in a highly turbulent zone, can report wind angles (θ_U) that appear to be within its useful range. Identifying these situations cannot be done in isolation, instead requiring data from one or more other anemometers.

The procedure for selecting the anemometer(s) that are actually in their useful range, as opposed to merely indicating that they are, may depend on the specific bias profiles of a given ship. However, invalid ranges for anemometers are most commonly caused because they are leeward of some localized object or structure. In these cases the wind speed on the leeward sensors will be lower than those on the windward side. Therefore, the anemometer with the higher wind speed should be selected. This sort of procedure could easily be included in an automatic bias correction algorithm, provided the system had simultaneous access to all wind sensor sources.

7.4. Improving bias

In certain cases where ABM analysis has been performed, the results may show that there are relative wind angles for which no anemometer location can provide useful data — essentially creating blind spot(s) for wind measurement. A less severe result could be that some wind angles within the useful range determined by the ABM analysis may produce poor data in practice at sea. In these cases, if there is a requirement for accurate wind data (such as for aircraft operations), then there are several options for improving the bias profiles. These include:

- Modifying superstructure features to improve flow quality;
- Re-locating anemometers to more favourable positions;
- Adding additional anemometers to less biased positions;
- Improving the anemometer (sensor type, alignment, calibration, etc.); or
- Applying appropriate constraints on wind-sensitive operations for conditions affected by blind spots or poor/unreliable data.

All of these approaches have different merit and feasibility considerations depending on the application.

7.5. True wind

Although the true wind, $\vec{T}$, is often treated as a given in most diagrams, for a ship at sea it is not measured directly. As the true wind can be determined using the anemometer measurements, bias in the relative wind will result in a biased assessment of the true

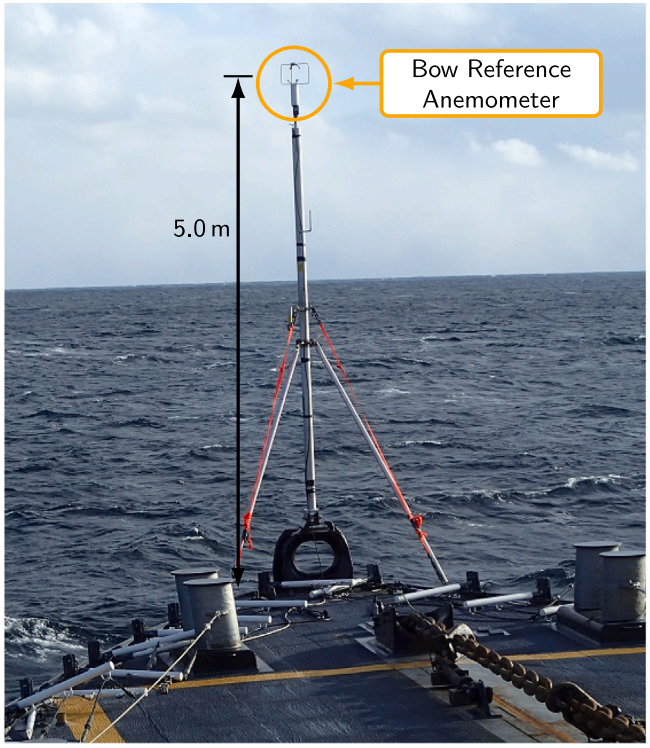

Fig. 15. Bow reference anemometer used on the sea trial.

wind. Therefore, the following steps, based on Eq. (4) re-arranged for Eq. (15), can be used to calculate the true wind vector using the corrected anemometer readings.

$$\vec{T} = \vec{U} - \vec{S} \tag{15}$$

1. Determine $\vec{S}$ using the ship's known speed, course, and heading;
2. Correct for anemometer bias (Section 7.3) to get an estimate of $\vec{U}$ from the measured relative wind $\vec{M}$; and
3. Use Eq. (15) to estimate $\vec{T}$ and Eq. (2) to convert between relative angles w.r.t. the ship, and absolute direction w.r.t. compass north.

8. Validating bias

When conducting model scale experiments or CFD simulations, it can be helpful to gain confidence in their results by validating them against real-world full scale data. This is best done on a dedicated sea trial on an appropriately instrumented ship. Such a trial was performed in 2017 as part of the anemometer bias study conducted for the Halifax Class frigates of the Royal Canadian Navy.

The primary difference in attempting to evaluate bias in a wind tunnel and on a ship at sea is that in a wind tunnel, the undistorted wind $\vec{U}$ is known and controllable. At sea, $\vec{U}$ cannot be measured directly from the ship because of the very anemometer bias that the trial is being conducted to evaluate. It may be possible to measure $\vec{T}$ using other sources such as buoys or small craft. In practice though, these are not always available and/or could overly constrain trial activities. Their use also introduces additional uncertainties.

Instead, the common approach is to temporarily fit the ship with additional reference anemometers for the trial. These reference sensors should be placed in areas where bias can be expected to be small, stable, and consistent. The bias metrics for a given target sensor can then be calculated using Eq. (16) with respect to a reference sensor as opposed to $\vec{U}$. Provided that the anemometer bias at the reference anemometer locations was also measured in the wind tunnel, then $\beta_{\theta R}$ and β_{VR} can be calculated and directly compared with the results from a sea trial.

$$\beta_{\theta R} = \bar{\theta}_M - \bar{\theta}_{MR} \tag{16a}$$

$$\beta_{VR} = \frac{\bar{M}}{\bar{M}_R} \tag{16b}$$

where,

- $\bar{\theta}_M$ is the mean measured relative wind angle of the target anemometer;
- $\bar{\theta}_{MR}$ is the mean measured relative wind angle of the reference anemometer;
- $\bar{M}$ is the mean measured 2D horizontal wind speed of the target anemometer;
- $\bar{M}_R$ is the mean measured 2D horizontal wind speed of the reference anemometer;
- $\beta_{\theta R}$ is the anemometer angle bias of the target anemometer w.r.t. to the reference anemometer;
- β_{VR} is the anemometer speed bias of the target anemometer w.r.t. to the reference anemometer.

A potential drawback of this approach is that if major differences were seen between the model and at-sea data, then it would not be obvious whether the differences were due to issues at the target, reference, or both anemometer locations. It is also possible that the two locations could have errors that cancel each other out. However, consistent agreement between multiple sensors over a range of conditions would be very strong evidence of validation.

Three reference sensors were used on the Halifax Class sea trial: at the bow, stern, and in front the mast. The bow reference anemometer, shown in Fig. 15, was attached to the top of a pole such that its measurement point was 5 m above the deck. Although ostensibly in clear air, wind tunnel results showed that the bow location still experienced biasing due to the ship hull. This bias was stable (except for tailwinds) making it a viable source for reference wind.

In addition to the extra reference sensors, two 3D ultrasonic anemometers were also fitted directly above the ship's existing propeller–vane anemometers. These were used to acquire higher resolution data, as well as to evaluate any potential benefit of moving the ship's anemometers to new, slightly higher, positions.

The trial consisted of performing straight track runs at constant speed for several minutes while logging data. The ship course was adjusted for each run to achieve a new relative wind angle; ship speed was set so as to maintain at least 15 knots of relative wind speed as measured by the windward reference ultrasonic anemometer.

Example results comparing data from the trial to the wind tunnel are given in Fig. 16. These are for the two ultrasonic anemometers temporarily fitted directly above the ship's port and starboard sensors using the bow anemometer as the reference wind. Wind tunnel data for the bow location was only measured out to beam winds as any wind coming from behind the ship would be heavily distorted — the figure is therefore limited from R90° through headwinds to G90°. The results show good agreement between the two sets of data. There appears to be a minor upward shift in the angular bias for the sea trial port anemometer compared with the wind tunnel, but this could be due an alignment issue of the ship's sensor. Small differences would be expected for the speed bias due to the effects of different vertical atmospheric velocity profiles as discussed in Section 5.2.

Various combinations of target and reference anemometers were examined and most showed good agreement between the sea trial and wind tunnel, with the exception of the ship's existing propeller–vane anemometers. Bias trends at these locations were not consistent with the wind tunnel nor the ultrasonics located directly above them. Various explanations were considered, such as whether the effect of vertical atmospheric velocity was more significant than the simplified adjustment discussed in Section 5.1 or whether the dynamic nature of

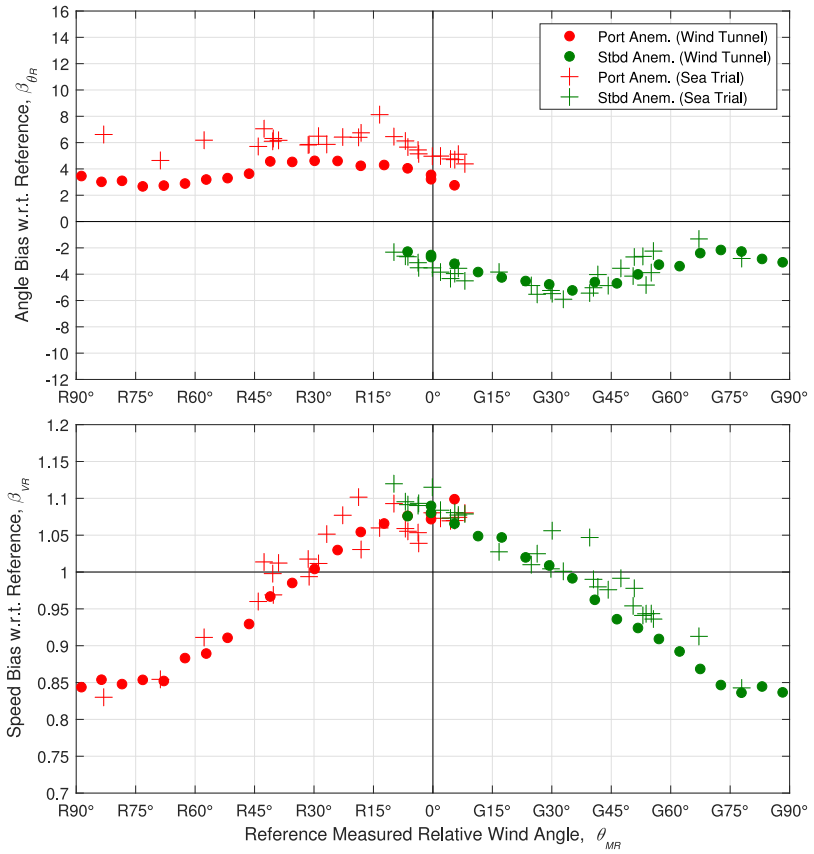

Fig. 16. Bias of mast port and starboard ultrasonic anemometers w.r.t. bow reference anemometer: sea trial and wind tunnels results.

the devices causes susceptibility to errors induced by ship motion. The issue has not been investigated further as the fleet's older propeller–vane units will soon be replaced by new ultrasonic units which have good agreement to wind tunnel data. Still, the unexpected behaviour of the propeller–vane sensors highlights the importance of performing full scale validation studies. Based on these sea trial results, new revised bias correction profiles, specifically tailored for the propeller–vane units, were created so they can be used until the ship anemometer upgrades are completed.

9. Conclusions

A ship and its structures create distortions that affect the accuracy of wind measurements made by its anemometers. Bias in wind readings is a particularly important issue for ships which operate aircraft. Although wind distortion cannot be eliminated, ship anemometer bias can be quantified and managed in a way that can restore the accuracy and usefulness of data. The ABM process first involves assessing the ship-induced bias present at actual or proposed anemometer locations using physical model testing or numerical simulation. Important considerations when performing these assessments are:

- Flow features that cause anemometer bias;
- Scaling and modelling necessary to ensure appropriate simulation;
- The impact of complicating real-world elements such as the ABL and ship motion;
- Anemometer type and its characteristics; and
- How information is displayed.

This paper provides definitions for the important quantities to consider in ABM and the concept of anemometer useful range. Following the process laid out in the paper, the resulting bias profiles for a given anemometer system can then be used to assess the proposed locations to determine whether they are sufficient to provide stable measurements for the full range of relative wind angles and whether the bias is severe enough to require real-time correction. A naval frigate was used as an example case to show this process using the bias profiles measured from wind tunnel testing. This data was then validated using full scale measurements from a dedicated sea trial.

Acronyms

ABL	atmospheric boundary layer
ABM	Anemometer Bias Management
APE	Anemometer Position Evaluation
AVT	Advanced Vehicle Technology
CFD	computational fluid dynamics
CSS	Canadian Survey Ship
JHSV	Joint High Speed Vessel
LES	large-eddy simulation
LHA	Amphibious Assault Ship (General Purpose)
NATO	North Atlantic Treaty Organization
NOC	National Oceanography Centre
NRC	National Research Council
RANS	Reynolds-averaged Navier–Stokes equations
RCN	Royal Canadian Navy
RMS	Root Mean Square
RV	Research Vessel
UK	United Kingdom
UR	useful-range
USN	United States Navy
USNS	United States Naval Ship
VOS	Voluntary Observing Ships
WMO	World Meteorological Organization

CRediT authorship contribution statement

Eric Thornhill: Conceptualization, Software, Validation, Formal Analysis, Investigation, Writing - original draft, Writing - review & editing. **Alanna Wall:** Conceptualization, Methodology, Validation, Formal Analysis, Investigation, Writing - review & editing. **Sean McTavish:** Investigation, Data curation, Writing - review & editing . **Richard Lee:** Investigation, Methodology.

Declaration of competing interest

The authors declare that they have no known competing financial interests or personal relationships that could have appeared to influence the work reported in this paper.

References

Augstein, E., Hoeber, H., Krügermeyer, L., 1974. Errors of temperature, humidity, and wind speed measurements on ships in tropical latitudes. Meteor Forsch.sergeb. (Berl.) Reihe B (9), 1–10.

AVT-217 Task Group, 2015. Modeling and Simulation of the Effect of Ship Design on Helicopter Launch and Recovery. STO technical report, NATO Research and Technology Organization.

Blanc, T.V., 1986a. Superstructure Flow Distortion Corrections for Wind Speed and Direction Measurements Made from Tarawa Class (LHA1-LHA5) Ships. NRL Report 9005, Naval Research Laboratory, Washington, D.C..

Blanc, T.V., 1986b. The effect of inaccuracies in weather-ship data on bulk-derived estimates of flux, stability and sea-surface roughness. J. Atmos. Ocean. Technol. 3 (1), 12–26.

Blanc, T.V., 1987. Superstructure Flow Distortion Corrections for Wind Speed and Direction Measurements Made From VIRGINIA Class (CGN38-CGN41) Ships. Tech. rep., Naval Research Laboratory, Washington, D.C..

Blanc, T.V., Larson, R.E., 1989. Superstructure Flow Distortion Corrections for Wind Speed and Direction Measurements Made from NIMITZ Class (CVN68-CVN73) Ships. NRL Report 9215, Naval Research Laboratory, Washington, D.C..

Blunt, D.M., 1991. Relative Wind Measurements on an FFG-7 Class Frigate (U). Technical Memorandum 447, DSTO Aeronautical Research Laboratory, Australian Department of Defence.

Bogorodskiy, M.M., 1966. A comparison of gradient observations of wind velocity by means of the froude spear-buoy and a shipboard gradient installation. Oceanol. Acad. Sci. USSR 6, 283–288.

Ching, J.K.S., 1976. Ship's influence on wind measurements determined from BOMEX mast and boom data. J. Appl. Meteorol. 15 (1), 102–106.

Davenport, A., 1960. Rationale for determining design wind velocities. Amer. Soc. Civil Eng. J. Struct. Div. 86, 39–68.

Elliot, J.A., 1981. Anemometer Blockage on CSS Dawson. AOL Research Notes No. 1, Atlantic Oceanographic Laboratory, Bedford Institute of Oceanography, Dartmouth, Nova Scotia, Canada B2Y 4A2, p. 14.

Forand, J., 2018. The LWKD Surface Boundary Layer Model: Version 8.10. Technical Memorandum DRDC Valcartier TM 2007-467, DRDC Valcartier.

Healey, J.V., 1992. Establishing a database for flight in the wakes of structures. J. Aircr. 29 (4), 559–564.

Hoeber, H., 1977. Accuracy of meteorological observations on the ocean. Seewart (Hambg.) (38), 204–213.

Irwin, H.P.A.H., 1979. Design and Use of Spires for Natural Wind Simulation. Laboratory Technical Report LTR-LA-233, National Research Council of Canada.

Kahma, K., Leppäranta, M., 1981. On errors in wind speed observations on R/V aranda. Geophysica 17 (1–2), 155–165.

Kidwell, K.B., Seguin, W.R., 1978. Comparison of Mast and Boom Wind Speed and Direction Measurements on U.S. GATE B-Scale Ships. Tech. rep., National Oceanic and Atmospheric Administration, Technical Report.

Mazzarella, D., 1954. Wind tunnel tests on seven aerovanes. Rev. Sci. Instrum. 25 (1), 63–68.

Moat, B.I., 1994. Improving Wind Velocity Measurements on Ships: Industrial Training Year at the James Rennell Centre for Ocean Circulation, 12 Aug 1993-9 Sept 1994. James Rennell Centre for Ocean Circulation Internal Document.

Moat, B.I., 2003. Quantifying the Effects of Airflow Distortion on Anemometer Wind Speed Measurements from Merchant Ships (Ph.D. thesis). University of Southampton.

Moat, B.I., Molland, A.F., Yelland, M.J., 2004a. A Wind Tunnel Study of the Mean Airflow around a Simple Representation of a Merchant Ship. SOC Research and Consultancy Report 87, Southampton Oceanography Centre, Southampton, United Kingdom.

Moat, B., Yelland, M., 2005. Improving Wind Speed Measurements from Ships: Computational Fluid Dynamics Modelling. Prepared for Skipsteknisk AS, Naval Architects, Norway.

Moat, B.I., Yelland, M.J., 2009. Airflow Distortion at Anemometer Sites on the OWS Polarfront. National Oceanography Centre Southampton Internal Document No. 14, Southampton Oceanography Centre, Southampton, United Kingdom.

Moat, B.I., Yelland, M.J., Molland, A.F., 2004b. Possible biases in wind speed measurements from merchant ships. In: 5th International Colloquium on Bluff Body Aerodynamics and Applications. University of Ottawa, Ottawa, Canada, pp. 537–540.

Moat, B.I., Yelland, M.J., Molland, A.F., 2006a. Quantifying the airflow distortion over merchant ships. Part II: Application of the model results. J. Atmos. Ocean. Technol. 23 (3), 351–360.

Moat, B.I., Yelland, M.J., Pascal, R.W., Molland, A.F., 2005. An overview of the airflow distortion at anemometer sites on ships. Int. J. Climatol. 25 (7), 997–1006.

Moat, B.I., Yelland, M.J., Pascal, R.W., Molland, A.F., 2006b. Quantifying the airflow distortion over merchant ships. Part I: Validation of a CFD model. J. Atmos. Ocean. Technol. 23 (3), 341–350.

NATO, 1993. Standardized Wave and Wind Environments and Shipboard Reporting of Sea Conditions: STANAG 4194 Ed. 2. Tech. rep..

O'Sullivan, N., Landwehr, S., Ward, B., 2013. Mapping flow distortion on oceanographic platforms using computational fluid dynamics. Ocean Sci. 9 (5), 855–866.

O'Sullivan, N., Landwehr, S., Ward, B., 2015. Air-flow distortion and wave interactions on research vessels: An experimental and numerical comparison. Methods Oceanogr. 12, 1–17.

Pierson, W.J., 1990. Examples of, reasons for, and consequences of the poor quality of wind data from ships for the marine boundary layer: Implications for remote sensing. J. Geophys. Res. 95 (C8), 13313.

Polsky, S., Ghee, T., Butler, J., Czerwiec, R., 2011. Application of CFD to anemometer position evaluation: A feasibility study. In: 29th AIAA Applied Aerodynamics Conference. American Institute of Aeronautics and Astronautics, Honolulu, Hawaii.

Popinet, S., Smith, M., Stevens, C., 2004. Experimental and numerical study of the turbulence characteristics of airflow around a research vessel. J. Atmos. Ocean. Technol. 21 (10), 1575–1589.

Rahmstorf, S., 1989. Improving the accuracy of wind speed observations from ships. Deep Sea Res. A 36 (8), 1267–1276.

Reinsvold, A., 2013. Roll and Pitch Corrections for a Shipboard Anemometer (Ph.D. thesis). College of Saint Benedict / Saint John's University.

Taylor, P.K., Kent, E.C., Yelland, M.J., Moat, B.I., 1999. The accuracy of marine surface winds from ships and buoys. In: CLIMAR99 - WMO Workshop on Advances in Marine Climatology. Vancouver, Canada.

Thiebaux, M., 1990. Wind Tunnel Experiments to Determine Correction Functions for Shipboard Anemometers. Canadian Contractor Report of Hydrography and Ocean Sciences No. 36CA9000396, Bedford Institute of Oceanography, Dartmouth, Nova Scotia, Canada.

2019. Turbulent Flow Instrumentation, https://www.turbulentflow.com.au/.

Wilczak, J.M., Oncley, S.P., Stage, S.A., 2001. Sonic anemometer tilt correction algorithms. Bound.-Lay. Meteorol. 99 (1), 127–150.

Yelland, M.J., Moat, B.I., Pascal, R.W., Berry, D.I., 2002. CFD model estimates of the airflow distortion over research ships and the impact on momentum flux measurements. J. Atmos. Ocean. Technol. 19 (10), 1477–1499.

Zdravkovich, M.M., 1997. Flow Around Circular Cylinders, Vol. 1: Fundamentals. Oxfrord University Press.